Particle conservation in dynamical density functional theory

2016 J. Phys.: Condens. Matter 28 244024

(http://iopscience.iop.org/0953-8984/28/24/244024)

IOP Publishing Journal of Physics: Condensed Matter
J. Phys.: Condens. Matter **28** (2016) 244024 (5pp) doi:10.1088/0953-8984/28/24/244024

Particle conservation in dynamical density functional theory

Daniel de las Heras[1], Joseph M Brader[2], Andrea Fortini[1,3] and Matthias Schmidt[1]

[1] Theoretische Physik II, Physikalisches Institut, Universität Bayreuth, D-95440 Bayreuth, Germany
[2] Department of Physics, University of Fribourg, CH-1700 Fribourg, Switzerland
[3] Department of Physics, University of Surrey, Guildford GU2 7XH, UK

E-mail: delasheras.daniel@gmail.com, joseph.brader@unifr.ch, andrea.fortini@me.com and matthias.schmidt@uni-bayreuth.de

Received 1 October 2015, revised 26 November 2015
Accepted for publication 18 December 2015
Published 26 April 2016

Abstract

We present the exact adiabatic theory for the dynamics of the inhomogeneous density distribution of a classical fluid. Erroneous particle number fluctuations of dynamical density functional theory are absent, both for canonical and grand canonical initial conditions. We obtain the canonical free energy functional, which yields the adiabatic interparticle forces of overdamped Brownian motion. Using an exact and one of the most advanced approximate hard core free energy functionals, we obtain excellent agreement with simulations. The theory applies to finite systems in and out of equilibrium.

Keywords: dynamic density functional theory, particle conservation, canonical density functional

(Some figures may appear in colour only in the online journal)

Classical density functional theory (DFT) is a highly successful approach for the description of equilibrium phenomena in both inhomogeneous liquids and solids. Conventionally, the theory is formulated in the grand canonical ensemble, where besides the system volume V and the temperature T, the chemical potential μ is prescribed. The number of particles, N, fluctuates [1, 2]. However, fixing N in a finite system, as is done in the canonical ensemble, can be a much more appropriate representation of an experimental situation. Examples of such systems include colloidal clusters [3] and fluids confined to closed cavities [4, 5]. The differences between canonical and grand canonical results can be very significant, see e.g. [6].

In order to extend DFT to canonical systems, several insightful studies have been carried out, such as the perturbation approach of [4, 5] and recent work on system-size dependence [7]. Only very recently, an exact decomposition procedure was discovered [6], which allows to obtain e.g. canonical density profiles from minimization of a grand canonical functional. While the variational principle of DFT has been formulated in the canonical ensemble [8, 9], any explicit access to the canonical free energy functional is not available at present.

Dynamical density functional theory (DDFT) is an extension of DFT to time-dependent situations, where the underlying many-body system is governed by overdamped Brownian motion [10, 11]. The DDFT equation of motion has a drift-diffusion structure, in which the gradient of the local chemical potential drives the one-body density. The former is obtained as the functional derivative of the grand canonical free energy functional with respect to the density. This represents an adiabatic approximation, and captures spatially nonlocal correlation effects. There are a considerable number of successful applications of DDFT, as compared to simulations and experimental results, such as e.g. spinodal decomposition [11], driven colloids in polymer solutions [12], ultrasoft particles in external fields [13] and colloidal sedimentation [14]. However, the formulation confuses canonical and grand canonical concepts.

Despite the importance of choosing the correct ensemble, and the fact that the deviations of theoretical results from simulation data are often attributed to ensemble differences, we are not aware of any systematic work that would address this issue. Clarifying this situation has become of particular importance, as recently the 'super-adiabatic' forces, which are

the contributions that are not derivable from any (adiabatic) free energy, were shown to be highly non-trivial by explicit many-body simulations [15]. A recent variational approach was formulated that allows to obtain the 'missing' super-adiabatic forces from functional differentiation of a free power functional [16]. To construct theories of the super-adiabatic forces, which are in general both nonlocal in space and time, it is important to clarify the issue of ensemble difference.

In this special issue contribution we formulate the correct adiabatic dynamics, which consistently conserves the number of particles during the time evolution of the one-body density. This enables a systematic study of the dynamics of small systems and thus opens a path for the theoretical investigation of problems such as, e.g. cluster formation or dynamics under confinement. Moreover, we show that the internal adiabatic forces are governed by the canonical free energy functional F_N, and give an explicit method for constructing F_N.

First we recall some statistical mechanics. In equilibrium the grand partition function is

$$\Xi(\mu, V, T) = \sum_{N=0}^{\infty} \mathrm{e}^{\beta\mu N} Z_N(V, T), \tag{1}$$

where $\beta = 1/(k_\mathrm{B}T)$, with k_B the Boltzmann constant, and Z_N the canonical partition function of a system with N particles The thermodynamic grand potential is

$$\Omega_0 = -k_\mathrm{B}T \ln \Xi. \tag{2}$$

Equilibrium grand canonical density profiles, $\rho_\mu(\boldsymbol{r})$, are a direct result of the DFT minimization for given value of μ, and are related to the canonical profiles $\rho_N(\boldsymbol{r})$ via

$$\rho_\mu(\boldsymbol{r}) = \sum_N p_N(\mu)\rho_N(\boldsymbol{r}), \tag{3}$$

where the probability $p_N(\mu)$ of finding N particles at given chemical potential μ is

$$p_N(\mu) = \exp(\beta\mu N)\frac{Z_N}{\Xi(\mu)}. \tag{4}$$

The decomposition method of [6] amounts to choosing an appropriate set of values of the chemical potential, $\{\mu_1, \ldots \mu_{N_\mathrm{max}}\} \equiv \{\mu_n\}$ and regarding $p_N(\mu_n)$ as the (N, n) element of an $N_\mathrm{max} \times N_\mathrm{max}$ matrix, $\mathbf{P}$. Here N_max is an upper cutoff in (3) and the trivial case $N = 0$ has been removed [6]. The matrix $\mathbf{P}$ can be constructed from DFT results for $\Omega_0(\mu_n)$, obtained for all $\{\mu_n\}$, and solving the resulting system of linear equations (2) and (4) for the set Z_N and hence $p_N(\mu_n)$. The inverse matrix $\mathbf{P}^{-1}$, with elements $\mathbf{P}^{-1}_{Nn}$, can then be used to decompose any grand ensemble average into the underlying canonical contributions. For example, the canonical density profiles are given by

$$\rho_N(\boldsymbol{r}) = \sum_n \mathbf{P}^{-1}_{Nn}\rho_{\mu_n}(\boldsymbol{r}). \tag{5}$$

Access to the canonical free energy functional $F_N[\rho]$ is not presently available. In order to provide this, let $\rho(\boldsymbol{r})$ be an arbitrary trial canonical density profile, with fixed number of particles, $\int \mathrm{d}\boldsymbol{r}\rho(\boldsymbol{r}) = N$. We turn $\rho(\boldsymbol{r})$ into the target for an inversion procedure to find the corresponding external potential $V(\boldsymbol{r})$, that generates $\rho(\boldsymbol{r})$ in (canonical) equilibrium. Then by subtracting the external contribution to the canonical free energy, the value of the canonical intrinsic free energy functional, F_N, evaluated at $\rho(\boldsymbol{r})$, can be obtained via

$$F_N[\rho] = -k_\mathrm{B}T \ln Z_N - \int \mathrm{d}\boldsymbol{r}\rho(\boldsymbol{r})V(\boldsymbol{r}). \tag{6}$$

In order to find $V(\boldsymbol{r})$, we start with the grand canonical Euler–Lagrange equation:

$$\beta V(\boldsymbol{r}) = c^{(1)}_\mu(\boldsymbol{r}) + \beta\mu - \ln \rho_\mu(\boldsymbol{r}), \tag{7}$$

where $c^{(1)}_\mu(\boldsymbol{r})$ is the one-body direct correlation function for density profile $\rho_\mu(\boldsymbol{r})$ and we have set the irrelevant thermal wavelength to unity. We have developed the following efficient iteration scheme. We start with an initial guess $V^{(0)}(\boldsymbol{r})$ and define the ith iteration step via

$$\beta V^{(i)}(\boldsymbol{r}) = \beta V^{(i-1)}(\boldsymbol{r}) - \ln \rho(\boldsymbol{r}) + \ln \sum_n \mathbf{P}^{-1}_{Nn}\rho_{\mu_n}(\boldsymbol{r}), \tag{8}$$

which can be derived from inserting equation (3) into (7) and then inverting with (5). The terms in the sum in equation (8) are re-calculated at each step, using the decomposition procedure described above.

We first apply the method to a system of one-dimensional hard particles, for which the exact grand canonical (Helmholtz) intrinsic free energy functional $F[\rho_\mu]$ is known [17]. In order to provide a severe test of the canonical functional approach, we consider $N = 2$ particles of length σ confined between two identical hard walls separated by a distance $h = 4.9\sigma$ along the x-axis. In addition we apply a parabolic external potential $V_0(x) = (x - h/2)^2 k_\mathrm{B}T/\sigma^2$. First we find the equilibrium canonical profile $\rho_{N=2}(x)$ using equation (5). Next, we generate trial density profiles $\rho_\alpha(x)$ via a multiplicative perturbation: $\rho_\alpha(x) = A[1 + \alpha(x - h/2)^2]\rho_{N=2}(x)$, where A is a constant that normalizes the profile such that it contains two particles, and α determines the strength of the perturbation, see figure 1(a). The corresponding external potential $V_\alpha(\boldsymbol{r})$ is then obtained by the iterative method (8). In figure 1(b) we show results for $V_\alpha(x) - V_0(x)$ for a range of values of α. The value of the canonical free energy functional, $F_N[\rho_\alpha]$, follows from equation (6); the results are plotted in figure 1(c). As expected, the canonical free energy increases with the perturbation strength α, and it is completely different from the intrinsic Helmholtz grand canonical free energy [17], see the inset of figure 1(c) for $F[\rho_\alpha]$. Here $F[\rho_\alpha]$ consists of the ideal gas functional and Percus' excess free-energy functional evaluated at ρ_α.

In order to demonstrate the applicability of the method to more realistic systems, we consider a three-dimensional case of hard spheres confined in a hard spherical cavity. We employ one of the most advanced free energy functionals presently available, namely the tensorial White Bear II fundamental measure functional [18]. The agreement of the canonical density profiles, as compared to Monte Carlo simulation data, is remarkable, see figure 1(d). The inset of figure 1(d) shows the probabilities p_N as a function of μ.

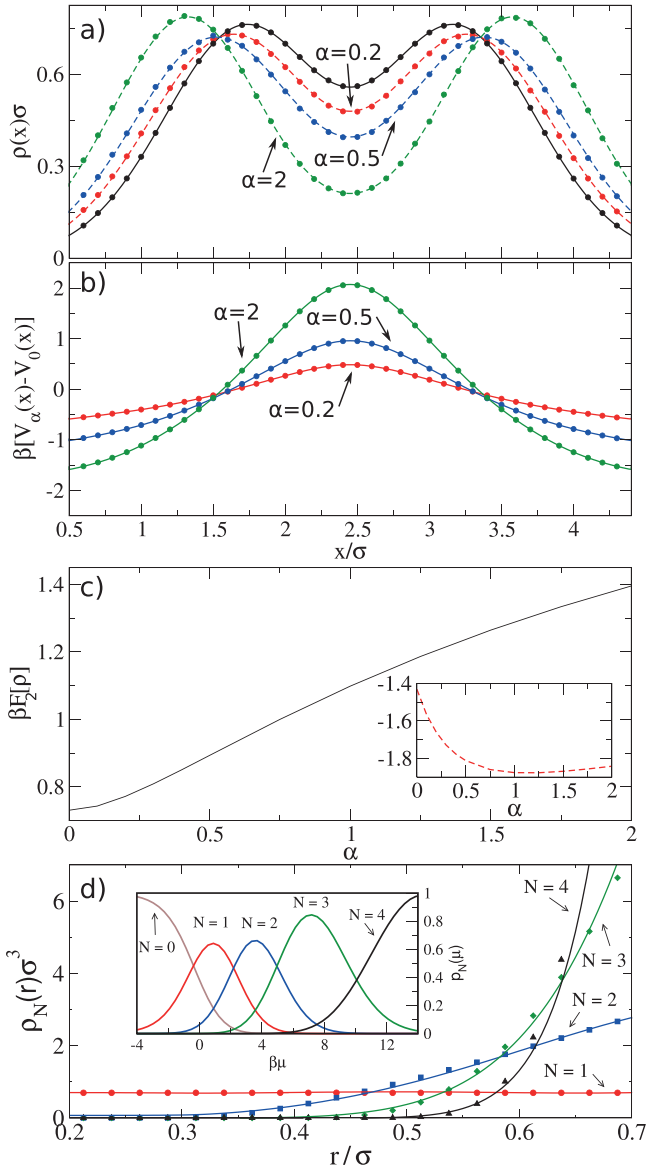

Figure 1. (a) Equilibrium density profile $\rho_{N=2}(x)$ (solid line) of a system of $N = 2$ hard rods confined in a slit pore and in presence of a parabolic external potential. The dashed lines are trial profiles obtained via $\rho(x) = \rho_{N=2}(x)A[1 + \alpha(x - h/2)^2]$ for different perturbation strengths α, as indicated. (b) Difference of scaled external potentials $\beta(V_\alpha(x) - V_0(x))$ for different values of α. Symbols in (a) and (b) correspond to Monte Carlo simulation, using the inversion procedure of [15] to obtain $V_\alpha(x)$. (c) Value of the canonical functional $\beta F_{N=2}$ and the intrinsic grand canonical free energy functional [17] (inset) evaluated at ρ as a function of the perturbation strength α. (d) Canonical density profiles of hard spheres confined in a spherical cavity of radius $r/\sigma = 1.2$. The solid lines are obtained via decomposition of the grand canonical functional White Bear mk. II [18]. Symbols represent Monte Carlo simulation data. The inset shows the probabilities p_N as a function of μ for $N = 1, 2, 3, 4$, as indicated.

The canonical equilibrium state serves as an initial condition for the time evolution. To describe the many-body dynamics, we employ the N-particle Smoluchowski equation [11], which locally conserves the particles throughout the time evolution (no exchange with any particle bath). An exact equation of motion for the time-dependent density profile $\rho_N(\boldsymbol{r}, t)$ is obtained by integrating over $N - 1$ degrees of freedom,

$$\frac{\partial \rho_N(\boldsymbol{r},t)}{\partial t} = D_0 \nabla \cdot [\nabla \rho_N(\boldsymbol{r},t) - \beta \mathbf{f}_N(\boldsymbol{r},t) - \beta \rho_N(\boldsymbol{r},t)(\mathbf{X}(\boldsymbol{r},t) - \nabla V_{\text{ext}}(\boldsymbol{r},t))], \tag{9}$$

where D_0 is the bare diffusion coefficient, $V_{\text{ext}}(\boldsymbol{r}, t)$ is a time-dependent external potential, $\mathbf{X}(\boldsymbol{r}, t)$ is a non-conservative force field, and $\mathbf{f}_N(\boldsymbol{r}, t)$ is the internal force density due to the interparticle interactions. The latter is given exactly by

$$\mathbf{f}_N(\boldsymbol{r},t) = -\int \mathrm{d}\boldsymbol{r}'\, \rho_N^{(2)}(\boldsymbol{r},\boldsymbol{r}',t) \nabla u(|\boldsymbol{r} - \boldsymbol{r}'|) \tag{10}$$

where $\rho_N^{(2)}(\boldsymbol{r}, \boldsymbol{r}', t)$ is the exact nonequilibrium pair density for N particles, and $u(r)$ is the interparticle pair potential. Schmidt and Brader [16] have shown that the internal force density can be systematically split into an adiabatic and a superadiabatic contribution,

$$\mathbf{f}_N(\boldsymbol{r},t) = \mathbf{f}_N^{\text{ad}}(\boldsymbol{r}, [\rho_N]) + \mathbf{f}_N^{\text{sup}}(\boldsymbol{r},t), \tag{11}$$

where the adiabatic force density is an instantaneous functional of the one-body density distribution and $\mathbf{f}_N^{\text{sup}}(\boldsymbol{r}, t)$ contains memory effects, which are neglected in DDFT. The adiabatic approximation corresponds to setting $\mathbf{f}_N^{\text{sup}}(\boldsymbol{r}, t) = 0$; a fundamental assumption of DDFT, which we retain in the present work. In contrast to DDFT, however, we will treat $\mathbf{f}_N^{\text{ad}}(\boldsymbol{r})$ exactly.

The instantaneous nonequilibrium density $\rho_N(\boldsymbol{r}, t)$ allows to define at each time t an adiabatic reference state as an equilibrium canonical ensemble of N particles with one-body density distribution

$$\rho_N^{\text{ad}}(\boldsymbol{r}) = \rho_N(\boldsymbol{r},t). \tag{12}$$

Here the left hand side (as well as all subsequent adiabatic quantities) is in general different at each time. We suppress this time dependence in the notation in order to highlight the static nature of the adiabatic state. The canonical inversion procedure (8) then determines the corresponding external ('adiabatic') potential, $V_{\text{ad}}(\boldsymbol{r})$, which, together with $u(r)$, specifies the adiabatic system completely. Note that $V_{\text{ad}}(\boldsymbol{r})$ is in general unrelated to $V_{\text{ext}}(\boldsymbol{r}, t)$ (as occurring in the equation of motion (9)). The corresponding canonical two-body density distribution $\rho_N^{(2)\text{ad}}(\boldsymbol{r}, \boldsymbol{r}')$ and the internal force density in the adiabatic system are related by

$$\mathbf{f}_N^{\text{ad}}(\boldsymbol{r}) = -\int \mathrm{d}\boldsymbol{r}' \rho_N^{(2)\text{ad}}(\boldsymbol{r},\boldsymbol{r}') \nabla u(|\boldsymbol{r} - \boldsymbol{r}'|). \tag{13}$$

In the following we demonstrate how $\mathbf{f}_N^{\text{ad}}(\boldsymbol{r})$ can be explicitly calculated. This specifies the adiabatic one-body dynamics completely. We present three different alternatives, all of which yield the same result.

(i) As the adiabatic system is in equilibrium, the net force vanishes. Hence the internal forces equal the negative external and entropic forces, and

$$\mathbf{f}_N^{\text{ad}}(\boldsymbol{r}) = \rho_N^{\text{ad}}(\boldsymbol{r}) \nabla [V_{\text{ad}}(\boldsymbol{r}) + k_{\text{B}} T \ln \rho_N^{\text{ad}}(\boldsymbol{r})]. \tag{14}$$

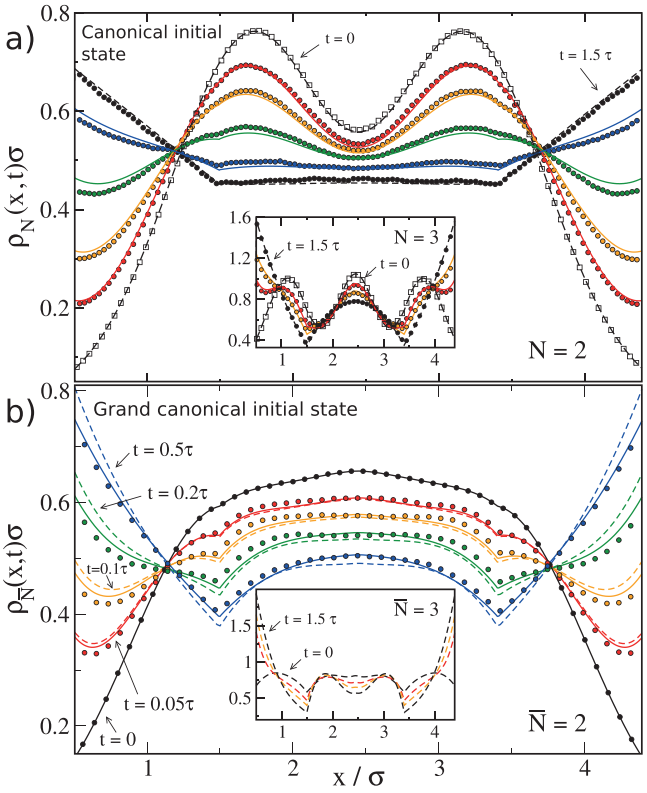

Figure 2. (a) Time evolution of canonical density profiles for a system of $N = 2$ and $N = 3$ (inset) particles in one dimension confined to a slit of width $h = 4.9\sigma$. For $t < 0$ the external potential consists of a harmonic trap $V_{\rm ext}(x) = (x - h/2)^2 k_{\rm B}T/\sigma^2$ and hard walls at $x = 0$ and $x/\sigma = 4.9$ (such that the density is cut at $x/\sigma = 0.5$ and 4.4). At $t = 0$ the harmonic trap is switched off and the density relaxes. The density at $t = 0$ and $t = 1.5\tau$ are given by the dashed lines, as indicated; the time scale is $\tau = \sigma^2/D_0$. At $t = 1.5\tau$ the system has practically relaxed to the final equilibrium state. Intermediate nonequilibrium profiles are shown at times $t/\tau = 0.05, 0.10, 0.20, 0.40$ (for $N = 2$) and $t/\tau = 0.05, 0.10, 0.15$ (for $N = 3$) and are given by the full lines. Symbols indicate the results of Brownian dynamics simulations. (b) Same as panel (a), but for an initial grand canonical profile with average number of particles is $\overline{N} = 2$, according to DDFT (dashed lines), the particle conserving theory (solid lines) and Brownian dynamics simulation (symbols). Solid lines and symbols have been obtained by recomposition of canonical states according to equation (18). The initial state, for $t = 0$, is the same in all cases. At $t = 0.5\tau$ the system has almost relaxed to its final state. The inset in (b) shows the time evolution according to DDFT of a grand canonical profile with $\overline{N} = 3$.

Here all quantities on the right hand side are known: the adiabatic density $\rho_N^{\rm ad}(\boldsymbol{r})$ via (12), and $V_{\rm ad}(\boldsymbol{r})$ has already been obtained from the canonical inversion procedure.

(ii) Functional differentiation of the canonical excess (over ideal gas) free energy functional $F_N^{\rm exc}[\rho]$ yields

$$\mathbf{f}_N^{\rm ad}(\boldsymbol{r}) = -\rho_N^{\rm ad}(\boldsymbol{r})\nabla \frac{\delta F_N^{\rm exc}[\rho]}{\delta\rho(\boldsymbol{r})}\bigg|_{\rho(\boldsymbol{r})=\rho_N^{\rm ad}(\boldsymbol{r})}. \tag{15}$$

In practice this procedure requires performing the functional derivative numerically.

(iii) From decomposition of the force in an adiabatic grand canonical state one obtains

$$\mathbf{f}_N^{\rm ad}(\boldsymbol{r}) = k_{\rm B}T\sum_n \mathbf{P}^{-1}_{Nn}\rho_{\mu_n}(\boldsymbol{r})\nabla c^{(1)}_{\mu_n}(\boldsymbol{r}), \tag{16}$$

where $\rho^{\rm ad}_{\mu_n}(\boldsymbol{r})$ is a set of grand canonical density profiles in the adiabatic potential $V_{\rm ad}(\boldsymbol{r})$, and $c^{(1)}_{\mu_n}(\boldsymbol{r})$ are the corresponding one-body direct correlation functions. Equation (16) can be derived from the exact grand canonical sum rule

$$k_{\rm B}T\rho_\mu(\boldsymbol{r})\nabla c^{(1)}_\mu(\boldsymbol{r}) = -\int {\rm d}\boldsymbol{r}'\rho^{(2){\rm ad}}_\mu(\boldsymbol{r},\boldsymbol{r}')\nabla u(|\boldsymbol{r}-\boldsymbol{r}'|), \tag{17}$$

and decomposing the grand canonical two-body density $\rho^{(2){\rm ad}}_\mu(\boldsymbol{r},\boldsymbol{r}')$ in the adiabatic system.

We have explicitly verified that the three methods yield the same results within numerical accuracy.

We are now in a position to integrate equation (9) in time using purely canonical forces to drive the dynamics. The adiabatic potential is re-calculated at each time step. In figure 2(a) we show results from the particle conserving theory for the relaxation of $N = 2$ and $N = 3$ (inset) hard rods, following the switching-off of a harmonic potential. The rods remain confined between two hard walls for all times and each system relaxes to its final (canonical) equilibrium state. The theoretical results are in very good agreement with our Brownian Dynamics simulation results (simulation details can be found in [15]).

The theoretical time evolution is slightly ahead of the simulation data. This is consistent with the direction of the super-adiabatic forces, which we have obtained by simulations, following the method of [15]; these results will be presented elsewhere. For the dense state $N = 4$ we also find very good agreement of theoretical results and simulation data (not shown). Any systematic deviations of theoretical results from the simulation data are entirely due to the omission of super-adiabatic forces in the theory, and not due to ensemble differences. For $N = 1$ the theory is exact, as the super-adiabatic forces vanish.

It is now straightforward to generalize to grand canonical initial conditions. Let the system at the initial time $t = 0$ be specified by a grand canonical density distribution $\rho^{(0)}_\mu(\boldsymbol{r})$ with average number of particles $\overline{N} = \sum_N N p^{(0)}_N(\mu)$. This state can be viewed as being composed of a set of underlying canonical density profiles $\rho^{(0)}_N(\boldsymbol{r})$ with statistical weights $p^{(0)}_N(\mu)$. Each of these canonical states evolves in time under particle conserving dynamics. Hence the entire grand canonical initial state evolves as a superposition of the trajectories $\rho_N(\boldsymbol{r}, t > 0)$. The statistical weights, however, are those of the initial grand canonical state, $p^{(0)}_N(\mu)$, as the system is decoupled from any particle bath for $t > 0$ (there is no source term in (9)). Hence the one-body density of this system is given by

$$\rho_{\overline{N}}(\boldsymbol{r}, t) = \sum_N p^{(0)}_N(\mu)\rho_N(\boldsymbol{r}, t). \tag{18}$$

Figure 2(b) shows corresponding results for $\overline{N} = 2$ and $\overline{N} = 3$ (inset). We find again very good agreement between the theory and BD simulation data. The theoretical time

evolution is slightly ahead of the BD data, which is entirely due to having neglected super-adiabatic forces in the theory. The theory captures the correct long-time limit. The time evolution of these initially grand canonical states differs very significantly from that of the corresponding canonical initial states, shown in figure 2(a). This striking discrepancy occurs despite the fact that $\overline{N} = N$, which highlights the importance of correct choice of ensemble in finite systems.

We next compare our approach to DDFT. As demonstrated by Archer and Evans [11], DDFT amounts to employing the equilibrium sum rule (17) for expressing the interaction force in terms of the one-body direct correlation function in the grand ensemble. However, instead of using the correct relation (12), DDFT amounts to constructing a grand canonical adiabatic state, with density distribution

$$\rho_\mu^{\mathrm{ad}}(\boldsymbol{r}) = \rho_N(\boldsymbol{r}, t). \tag{19}$$

Via the Euler–Lagrange equation (7), a corresponding external potential exists, that generates $\rho_\mu^{\mathrm{ad}}(\boldsymbol{r})$ in the grand ensemble. The grand canonical adiabatic system under the influence of this external potential possess a two-body density, $\rho_\mu^{(2)}(\boldsymbol{r}, \boldsymbol{r}')$, for which using the sum rule (17) yields the associated force density

$$\mathbf{f}_{\mathrm{DDFT}}(\boldsymbol{r}) = -k_{\mathrm{B}}T\rho_\mu^{\mathrm{ad}}(\boldsymbol{r})\nabla c_\mu^{(1)}(\boldsymbol{r}), \tag{20}$$

which differs from the exact expression (16). In the example of figure 2(b), although DDFT deviates more strongly from the simulation data than the present theory, it nevertheless provides a reasonable description of the dynamics of an initial grand canonical state.

Although we have presented results for very simple test cases, the particle conserving dynamical theory is applicable to any system for which a grand canonical density functional is available. Studies of complex phenomena, such as the dynamics of colloidal cluster formation, or transport through ion channels are thus within reach. As exemplified by the comparison of figures 2(a) and (b), the time evolution of a system containing only a few particles is very sensitive to the choice of ensemble. In systems with a reduced number of particles the use of a canonical DFT and particle conserving dynamics is indispensable in order to compare with experiments or simulations performed at fixed particle number. Canonical and grand canonical ensembles are equivalent in the thermodynamic limit, and the time evolution in DFT is just a temporal sequence of equilibrium states. Hence, one might expect our particle conserving theory and (standard) DDFT to be equivalent in systems with a large number of particles. However, local fluctuations typically involve only a reduced number of particles. Therefore, the dynamics of localized phenomena might depend on the ensemble, even in the thermodynamic limit. This is an open problem to be addressed in future work.

Acknowledgments

DdlH and JMB contributed equally to this work.

References

[1] Evans R 1979 The nature of the liquid-vapour interface and other topics in the statistical mechanics of non-uniform, classical fluids *Adv. Phys.* **28** 143–200
[2] Mermin N D 1965 Thermal properties of the inhomogeneous electron gas *Phys. Rev.* **137** A1441
[3] Meng G, Arkus N, Brenner M P and Manoharan V N 2010 *Science* **327** 560
[4] González A, White J A, Román F L, Velasco S and Evans R 1997 Density functional theory for small systems: hard spheres in a closed spherical cavity *Phys. Rev. Lett.* **79** 2466
[5] White J A, González A, Román F L and Velasco S 2000 Density-functional theory of inhomogeneous fluids in the canonical ensemble *Phys. Rev. Lett.* **84** 1220
[6] de las Heras D and Schmidt M 2014 Full canonical information from grand-potential density-functional theory *Phys. Rev. Lett.* **113** 238304
[7] Chakraborty D, Dufty J and Karasiev V V 2015 System-size dependence in grand canonical and canonical ensembles *Adv. Quant. Chem.* **71** 11
[8] Hernando J A and Blum L 2001 Density functional formalism in the canonical ensemble *J. Phys.: Condens. Matter* **13** L577
[9] Dwandaru W S B and Schmidt M 2011 Variational principle of classical density functional theory via Levy's constrained search method *Phys. Rev.* E **83** 061133
[10] Marconi U M B and Tarazona P 1999 Dynamic density functional theory of fluids *J. Chem. Phys.* **110** 8032
[11] Archer A J and Evans R 2004 Dynamical density functional theory and its application to spinodal decomposition *J. Chem. Phys.* **121** 4246
[12] Penna F, Dzubiella J and Tarazona P 2003 Dynamic density functional study of a driven colloidal particle in polymer solutions *Phys. Rev.* E **68** 061407
[13] Dzubiella J and Likos C N 2003 Mean-field dynamical density functional theory *J. Phys.: Condens. Matter* **15** L147
[14] Royall C P, Dzubiella J, Schmidt M and van Blaaderen A 2007 Nonequilibrium sedimentation of colloids on the particle scale *Phys. Rev. Lett.* **98** 188304
[15] Fortini A, de las Heras D, Brader J M and Schmidt M 2014 Superadiabatic forces in Brownian many-body dynamics *Phys. Rev. Lett.* **113** 167801
[16] Schmidt M and Brader J M 2013 Power functional theory for Brownian dynamics *J. Chem. Phys.* **138** 214101
[17] Percus J K 1976 Equilibrium state of a classical fluid of hard rods in an external field *J. Stat. Phys.* **15** 505
[18] Hansen-Goos H and Roth R 2006 Density functional theory for hard-sphere mixtures: the White Bear version mark II *J. Phys.: Condens. Matter* **18** 8413